

Modeling aquifer systems with analytic elements and subdomains

C. R. Fitts¹

Received 25 June 2009; revised 27 February 2010; accepted 5 March 2010; published 16 July 2010.

[1] A new approach for analytic element (AE) modeling of groundwater flow is presented. The approach divides the modeled region into polygonal subdomains, each with its own analytic flow model and its own local isotropic or anisotropic aquifer parameters. This allows analytic modeling of systems where the anisotropy ratio and direction vary spatially, an AE capability not possible without subdomains. It also allows for flexible layering in a model, with more layers in the area of interest abutting fewer layers in the far field. The approach is demonstrated in a model with seven subdomains and a mix of single-layer and triple-layer areas. Checks of the model indicate that the inter-subdomain boundary conditions can be approximated well, and where the differential equation is approximated (multilayer areas and transient flow), that approximation can be quite accurate.

Citation: Fitts, C. R. (2010), Modeling aquifer systems with analytic elements and subdomains, *Water Resour. Res.*, 46, W07521, doi:10.1029/2009WR008331.

1. Introduction

[2] The analytic element method for groundwater flow modeling is based on superposition of analytic functions to yield a composite solution that can closely approximate a variety of boundary conditions. The method, originally developed by *Strack* [1989, 2003] and described by *Haitjema* [1995] and *Fitts* [2002], fills a niche role in groundwater modeling between the simple geometries solved by exact analytic solutions and the highly heterogeneous, multilayered geometries that are usually solved with numerical methods like finite elements or finite differences.

[3] Analytic element (AE) approaches are appealing because the domain is not discretized into a grid or mesh of elements, but instead only boundaries of the domain are discretized. As a result, AE models tend to have simpler input requirements and excel at simulating small-scale detail within a much larger scale model. The system of equations in AE models typically generates a coefficient matrix that is fully-populated. Adding heterogeneity adds equations to the system. By contrast, numerical methods generate a narrow banded coefficient matrix, and the number of equations depends on the mesh or grid size, not on the amount of heterogeneity. Efficient iterative solvers for large banded matrices and the lack of computational penalty for heterogeneity are key factors that favor numerical methods for very complex problems. However, numerical methods have their drawbacks. They require fine discretization close to features like wells or drains, have less geometric flexibility, and can require considerable effort when it is necessary to alter the grid or mesh.

[4] The approach presented here provides novel AE capabilities for simulating heterogeneous and anisotropic

aquifers in a general way. This is accomplished by decomposing the modeled region into subdomains, each with its own separate AE model [*Fitts*, 2004]. The direction and ratio of anisotropy are homogeneous within a subdomain, but may vary from one subdomain to another, even within the same layer. Each subdomain model consists of expressions for head, potential, and discharge that only include terms contributed by elements inside the subdomain or on its boundary; elements beyond the boundary don't contribute directly.

[5] Traditional AE techniques have treated a model layer as an infinite planar domain, with each analytic element in a given layer contributing terms to the potential and aquifer discharge functions throughout that layer. Infinite-domain AE models typically define a heterogeneity with an internal polygonal boundary, using line doublet elements to represent the boundary segments [*Strack and Haitjema*, 1981; *Fitts*, 1985]. If a layer contains many heterogeneities and other boundary conditions, the number of terms in the potential and discharge equations becomes large. To reduce this computational burden, *Strack et al.* [1999] and *Craig et al.* [2006] employ a scheme known as "superblocks", where a layer is divided into a grid of rectangular blocks, and series expansion approximations are substituted for direct evaluation of functions for elements outside of each block. Superblocks work well to reduce the computation involved in evaluating these functions, but they add some computational overhead and they rely on convergence of an iterative block-by-block solution process.

[6] With the approach presented here, there is some computational savings because each subdomain model has equations with relatively few terms - just terms from elements on the subdomain boundary or within it. One consequence of using subdomains is that assembling the system of equations is quicker, as each equation in the system depends on a subset, rather than all, of the other elements. Likewise, computation of heads or discharges is rapid once a solution is determined.

¹Geosciences Department, University of Southern Maine, Gorham, Maine, USA.

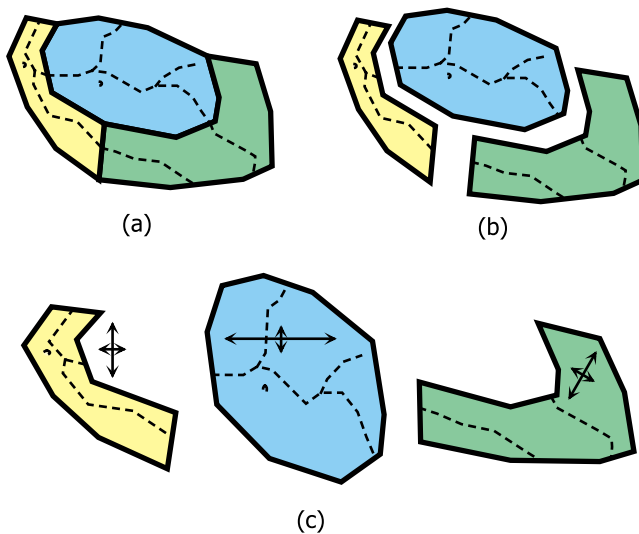


Figure 1. (a) Example model with three subdomains. (b) Three separate subdomain models shown separated. (c) Subdomain models in transformed \hat{Z} coordinates, with principal hydraulic conductivities shown with arrows. Elements on subdomain boundaries are shown with solid lines and elements interior to subdomains are shown with dashed lines.

[7] Infinite-domain AE approaches have already been extended to model horizontal anisotropy using a coordinate transformation that is commonly employed with anisotropic flow nets [Muskat, 1937]. Bakker and Hemker [2002] adapted AE for flow in multilayer systems with anisotropy in each layer and Fitts [2006] adapted AE to simulate flow near a well in a single layer with anisotropy. A limitation of these global coordinate transformations is that the direction and ratio of the anisotropy must be uniform throughout an entire layer. The approach described here provides more versatile anisotropy capabilities, allowing various subdomains in the same layer to have differing anisotropy ratios and principal directions.

[8] Another benefit of this approach is that it is possible to transition the model layering scheme across subdomain boundaries. For example, a model could consist of a single layer in the far field, but have a multilayer stack of subdomains in the area of interest. Such an example is presented at the end of this paper. This flexibility with layering efficiently concentrates the model detail and computational effort where it is most needed.

[9] Bakker [2006a, 2006b] presented AE techniques that allowed modeling of multiple layers with heterogeneity, using a mix of infinite-domain and subdomain AE approaches. His techniques result in exact distributions of inter-layer leakage and exact solution of the governing differential equations, which are only approximated by the technique presented here. His techniques are restricted to confined isotropic aquifers, steady flow, and a limited suite of analytic elements (wells, constant-strength linesinks, circular areas of constant recharge, and cylindrical heterogeneities). The techniques of Bakker [2006a, 2006b] achieve perfect continuity of the comprehensive flow (summed over all layers), but the normal component of flow across heterogeneity boundaries of individual layers is approximated

and matched only at collocation points. The technique presented here also approximates continuity of flow at inter-domain boundaries, but it matches discharge across intervals rather than matching the normal component of flow at collocation points.

[10] Dividing the modeled region into entirely separate subdomain models has not been done before with AE, but it has been a common approach in boundary element (BE) methods. Liggett and Liu [1983] and Bruch and Lejeune [1989] applied subdivision to heterogeneous and anisotropic porous media flow. Shiah *et al.* [2006] applied subdivision and coordinate transformation to simulate heterogeneous and anisotropic heat conduction in both two and three dimensions. For models with no internal sources/sinks, both AE and BE models boil down to distributions of sinks and dipoles along the external model boundary. Most boundary element approaches assume sink or dipole distributions with one, two, or three degrees of freedom per line segment and in many cases BE line integrals are approximated with numerical integration [Beer *et al.*, 2008; Kythe, 1995]. In contrast, AE models use analytic expressions for the sink and dipole distributions and line elements can have ten or more degrees of freedom [Jankovic and Barnes, 1999]. The normal component of flow between adjacent subdomains in BE models is matched at collocation points only [Beer *et al.*, 2008; Liggett and Liu, 1983], so there is no guarantee of overall flow continuity. As discussed later in this paper, the AE approach presented here does preserve flow continuity over intervals along a line segment. In cases with spatially-variable areal extraction, BE methods generally discretize the extraction distribution and numerically integrate the domain part of the integral equation [Beer *et al.*, 2008; Kythe, 1995].

2. Subdomain Equations

[11] The mathematical model consists of separate two-dimensional AE models for each polygonal subdomain, each of which has its own unique, constant aquifer parameters including base and top elevations, and hydraulic conductivity. The hydraulic conductivity in the plane of the subdomain may be anisotropic, and the anisotropy direction and ratio can vary from one subdomain to another. Consider the hypothetical single-layer model with three subdomains illustrated in Figure 1. The mathematical model for each subdomain consists of equations for the potential and aquifer discharge vector as functions of space, with terms contributed by all elements within the subdomain and line

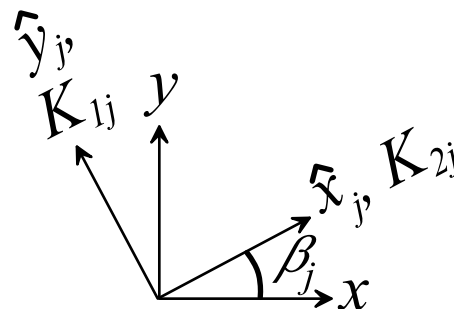


Figure 2. Coordinate systems for an anisotropic subdomain.

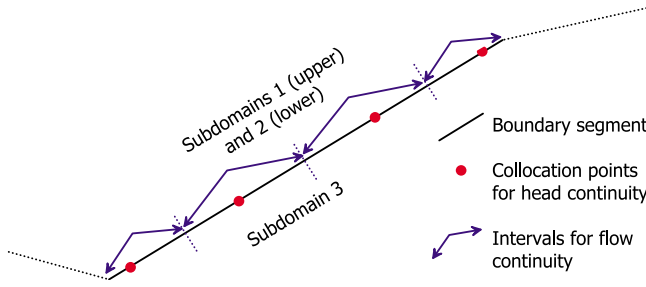


Figure 3. Boundary conditions along an inter-subdomain boundary line segment.

elements on its boundary. Along shared boundaries between subdomains, there are strings of linesink elements with separate strength parameters – one string for each subdomain. The strengths of these inter-subdomain line elements are determined by requiring continuity of head and continuity of normal flux at the boundary, as discussed in the following section.

[12] Location within the global two-dimensional x, y coordinate system of the model is defined with the complex variable $z = x + iy$. For each anisotropic subdomain, two additional coordinate systems are employed. The \hat{z}_j plane represents a rotated coordinate system for the j th subdomain, where the \hat{x}_j axis aligns with the subdomain's minor principal hydraulic conductivity K_{2j} , and the \hat{y}_j axis aligns with its major principal conductivity K_{1j} .

$$\hat{z}_j = \hat{x}_j + i\hat{y}_j = ze^{-i\beta_j} \quad (1)$$

where β_j is the angle between the x axis and the \hat{x}_j axis (Figure 2). The \hat{Z}_j plane represents a rotated and stretched coordinate system which creates an equivalent isotropic subdomain where the usual analytic element functions may be superposed (Figure 1).

$$\hat{Z}_j = \hat{X}_j + i\hat{Y}_j = \sqrt{K_{1j}/K_{2j}} \hat{x}_j + i\hat{y}_j \quad (2)$$

Similar coordinate transformations are commonly used in analytic solutions for anisotropic media [e.g., *Muskat*, 1937; *Bear*, 1972]. The equivalent isotropic conductivity that applies in the \hat{Z}_j plane is

$$\hat{K}_j = \sqrt{K_{1j}K_{2j}} \quad (3)$$

For an isotropic subdomain, $\hat{Z}_j = z$ and $\hat{K}_j = K_{1j} = K_{2j}$.

[13] The equation for the discharge potential $\Phi_j(\hat{Z}_j)$ [L^3/T] in the j th subdomain is the sum of AE potential functions written in terms of \hat{Z}_j coordinates. Individual potential functions are either solutions of the Laplace equation (well and line elements) or solutions of the Poisson equation (areal extraction elements), and their sum is a solution of the Poisson equation:

$$\nabla^2 \Phi_j = \frac{\gamma}{\sqrt{K_{1j}K_{2j}}} \quad (4)$$

where γ is the net extraction per area [L/T] in terms of the real x, y coordinates. The extraction γ is a distributed sink

term that may have contributions from leakage out the top (L_t), leakage out the bottom (L_b), and flux into storage:

$$\gamma = L_t + L_b + S \frac{\partial h_j}{\partial t} \quad (5)$$

where S is storativity (confined) or specific yield (unconfined), h_j is head in subdomain j and t is time. To simulate transient flow, finite difference time steps are used to approximate the storage term:

$$\gamma = L_t + L_b + S \frac{\Delta h_j}{\Delta t} \quad (6)$$

where Δh_j is the change in head over a time step of duration Δt . *Haitjema and Strack* [1985] previously blended AE with finite difference time steps in this way to model transient flow.

[14] The leakage terms L_t and L_b can be specified, as in the case of recharge in the uppermost model layer or leakage from the bottom model layer. Alternatively, they can be determined based on the head difference between the subdomain and heads above or below the subdomain. If the subdomain has leakage to an overlying surface water or another subdomain, $L_t = (h_j - h_t)C_t$ where h_t is the head above the subdomain, and C_t is a conductance term defined as

$$C_t = K_{vt}/d_t \quad (7)$$

where K_{vt} and d_t are the effective vertical hydraulic conductivity and thickness, respectively, between subdomain j and the overlying layer or surface water. Similar equations define L_b .

[15] If a model is steady state and L_t and L_b are specified and constant within a subdomain, γ is constant and the governing equation (4) may be satisfied exactly in the subdomain by using one constant strength areal extraction element (e.g., equation 9.15 of *Strack* [1989]). On the other hand, if a model is transient or the subdomain has spatially-

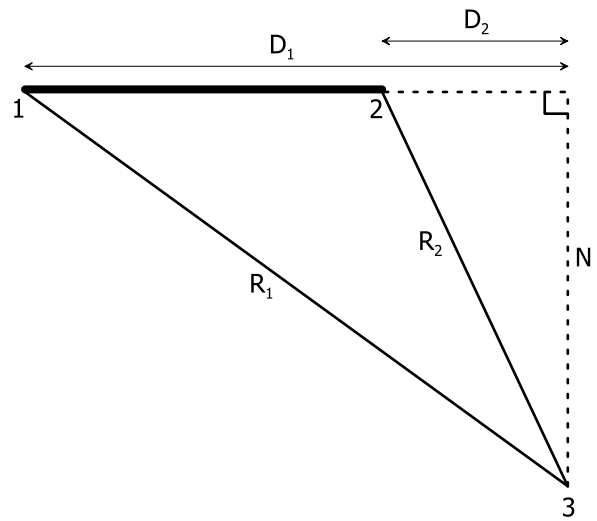


Figure 4. Geometry for flow continuity expressions over an interval 1–2 of a line segment. Point 3 is the location of a spatially variable extraction basis point or the central point of the constant extraction term.

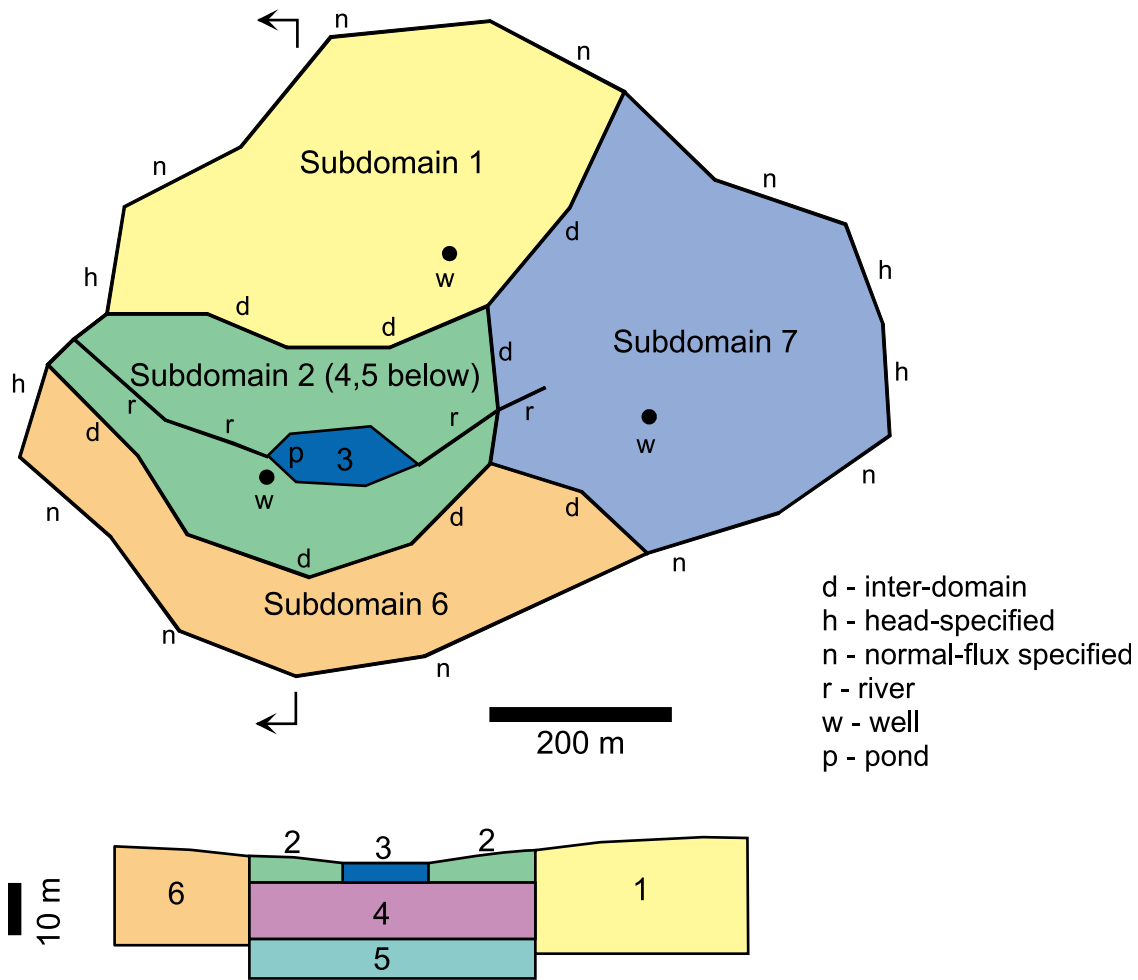


Figure 5. Example model layout in (top) plan view and (bottom) cross section.

variable L_t or L_b , the governing equation is only approximated, here using the spatially-variable extraction elements described by *Strack and Jankovic* [1999] to create a distribution $\gamma(\hat{Z}_j)$ that approximates the right hand side of equation (6).

[16] The typical potential-head relations are used: $\Phi_j = \hat{K}_j b_j h_j$ for a confined subdomain of thickness b_j and $\Phi_j = (1/2)\hat{K}_j(h_j - d_j)^2$ for an unconfined subdomain with base elevation d_j . With these definitions, Φ_j is a discharge potential in the \hat{Z}_j plane and the following equations are valid.

$$\frac{\partial \Phi_j}{\partial \hat{X}_j} = -Q_{\hat{X}_j} \quad \frac{\partial \Phi_j}{\partial \hat{Y}_j} = -Q_{\hat{Y}_j} \quad (8)$$

where $Q_{\hat{X}_j}, Q_{\hat{Y}_j}$ [L^2/T] are the components of the horizontal discharge vector integrated over the saturated aquifer thickness.

[17] Using equations (2), (3), and (8) it can be shown that

$$Q_{\hat{x}_j} = Q_{\hat{X}_j}, \quad Q_{\hat{y}_j} = \sqrt{K_{1j}/K_{2j}} Q_{\hat{Y}_j} \quad (9)$$

The discharge vector in global coordinates is determined by evaluating equations (8) and (9) in sequence, and then the following equation

$$Q_x + iQ_y = (Q_{\hat{x}_j} + iQ_{\hat{y}_j})e^{i\beta_j} \quad (10)$$

3. Analytic Elements

[18] Each subdomain potential function $\Phi_j(\hat{Z}_j)$ is the sum of contributions from fundamental analytic elements plus a constant. All of the elements used here have been described elsewhere. The standard well element described by *Strack* [1989] is used in isotropic subdomains and the well element of *Fitts* [2006] is used in anisotropic subdomains. Line boundaries are represented by high-order linesink elements similar to those described by *Jankovic and Barnes* [1999].

[19] Spatially-variable extraction is modeled with the multiquadric radial basis function elements described by *Strack and Jankovic* [1999]. In their work, a polygon of line elements internal to an infinite domain bounds the extraction area, while here the extraction area boundary is the sub-

Table 1. Subdomain Properties

Subdomain	Type	Base Elevation (m)	Top Elevation (m)	Horizontal K (m/day)		Angle K ₁ to x Axis (deg)	Vertical K (m/day)	Storativity	Recharge (m/day)
				K ₁	K ₂				
1	Unconfined	-10		0.5	0.25	90		0.10	0.0004
2	Unconfined	10		3.0	1.5	0	0.3	0.10	0.0016
3	Confined	10	14	3.0	1.5	0	0.3	0.003	
4	Confined	-2	10	1.0	0.5	15	0.1	0.003	
5	Confined	-15	-2	5.0	1.0	30	0.4	0.003	
6	Unconfined	-8		0.8	0.2	-30		0.10	0.0006
7	Unconfined	-5		2.0	2.0			0.10	0.0010

domain external boundary. The contribution that extraction elements with n basis points make to Φ_j is

$$\Phi_{Ej} = \frac{1}{9} \sum_{i=1}^n b_{ij} r_{ij}^3 + \frac{1}{4} B_{0j} r_{0j}^2 \quad (11)$$

with the constraint that

$$\sum_{i=1}^n b_{ij} = 0 \quad (12)$$

where b_{ij} is the strength parameter associated with the i th basis point in subdomain j , r_{ij} is the radial distance in the \hat{Z} plane from the i th basis point to the point where Φ_j is evaluated, B_{0j} is an average extraction rate in subdomain j , and r_{0j} is the radial distance in the \hat{Z} plane from a centrally-located point in the subdomain (\hat{Z}_{0j}) to the point where Φ_j is evaluated. Equation (12) assures that the net contribution of the summation in equation (11) tends to zero and extraction approaches B_{0j} far from the basis points.

[20] The modeled extraction rate γ in subdomain j is

$$\gamma = \sqrt{K_{1j}/K_{2j}} \nabla^2 \Phi_j = \sqrt{K_{1j}/K_{2j}} \left(\sum_{i=1}^n b_{ij} r_{ij} + B_{0j} \right) \quad (13)$$

The $n + 1$ strength parameters b_{ij} and B_{0j} are determined with equation (12) and collocation, equating the right sides of equations (6) and (13) at each basis point.

4. Inter-subdomain Boundary Conditions

[21] Two kinds of equations are generated at inter-subdomain boundaries: one for continuity of head and the other for continuity of flow. Continuity of head is enforced at collocation points on the shared boundary of adjacent subdomains. Continuity of flow is enforced across a series of consecutive intervals along each line segment on the common boundary. For example, consider one line segment along an inter-subdomain boundary that has subdomains 1 (upper) and 2 (lower) on the left, and subdomain 3 on the right (Figure 3). Each subdomain has a linesink element along this line, and each of these linesinks has four unknown strength parameters. Continuity of head is enforced at four collocation points, each with one equation setting $h_1 = h_2$ and another setting $h_1 = h_3$ for a total of 8 equations. There are four additional equations balancing the discharge across four intervals on the line segment: $\Delta Q_1 + \Delta Q_2 = \Delta Q_3$, where ΔQ_j is the discharge across the interval in the j th subdomain. There are a total of 12 equations to correspond with the 12 unknown strength parameters associated with

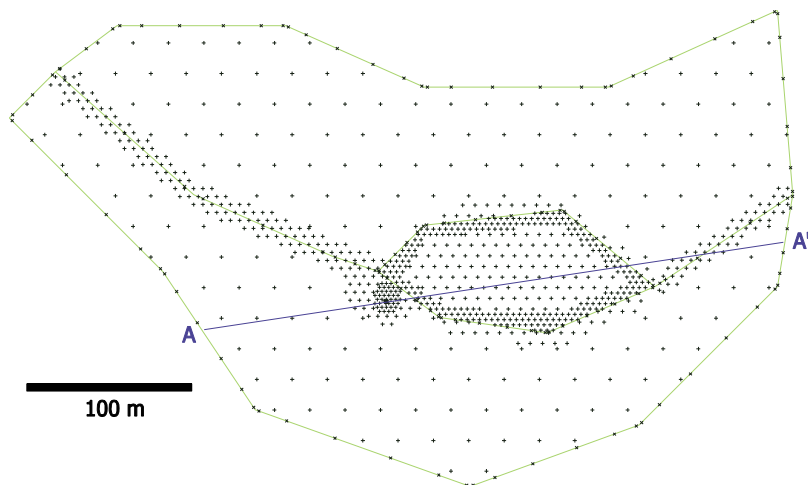


Figure 6. Location of extraction element basis points (+ symbols) and line element collocation points (x symbols) in the multilayer area of the model. Line elements shown in green. The section line A-A' relates to Figures 10 and 11.

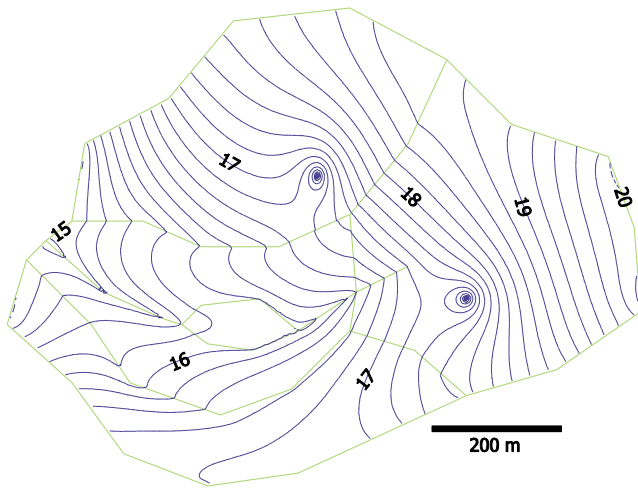


Figure 7. Model-simulated heads (blue) in entire modeled area, subdomains 1, 2, 3, 6, and 7 (upper layer in 3-layer area). Contour interval 0.2 m. Line elements shown in green.

the boundary linesinks in subdomains 1–3. The discharge-balancing equations guarantee total continuity of flow across each of the four intervals on the line segment, although there is only approximate continuity of the normal component of flow at any given point on the line segment. In other words, global mass balance is preserved over each interval, but locally normal flow components along the boundary may be discontinuous.

[22] The discharge across an interval in one subdomain is computed by summing the discharges contributed by each element in that subdomain. The well and line elements are represented by analytic complex potential functions, and their contribution to the discharge across an interval may be obtained from the difference in the stream function at the end points of the interval [Haitjema and Kelson, 1996]. For the extraction elements there is no stream function and the discharge across a line interval is computed using exact expressions derived for this purpose. Haitjema and Kelson [1996] presented an expression for a constant strength extraction element and Craig [2005] presented an expression for multiquadric extraction elements based on equations by Strack and Jankovic [1999]. Similar expressions were derived independently here, but without using coordinate systems local to the line segment as was done by Craig [2005] and Strack and Jankovic [1999]. The resulting equation for discharge across a line segment due to the extraction elements in subdomain j is

$$\Delta Q_{Ej} = \sum_{i=1}^n \frac{b_{ij}N_i}{6} \left[R_{1i}D_{1i} - R_{2i}D_{2i} + N_i^2 \ln \left(\frac{R_{1i} + D_{1i}}{R_{2i} + D_{2i}} \right) \right] + \frac{B_{0j}N_0}{2} (D_{10} - D_{20}) \quad (14)$$

where N , R , and D are lengths defined by the geometry of the line interval and extraction element (Figure 4).

5. Example Application

[23] The techniques described above have been implemented in a research program written in the C# language.

A steady state example model is presented first and then a transient variation on this model is shown.

[24] The model configuration is shown in Figure 5. There are 7 different subdomains in the model. Subdomains 1, 6, and 7 represent single-layer portions of the model that are farther from the area of interest. Subdomains 2–5 are the prime area of interest near a stream, pond, and well. This area has three model layers with leakage between the layers and leakage between the surface waters and underlying aquifer. Table 1 lists the properties of each subdomain. Subdomain 7 is the only isotropic subdomain; the other six are anisotropic with varying ratios and orientations. There are pumping wells in subdomains 1, 5, and 7.

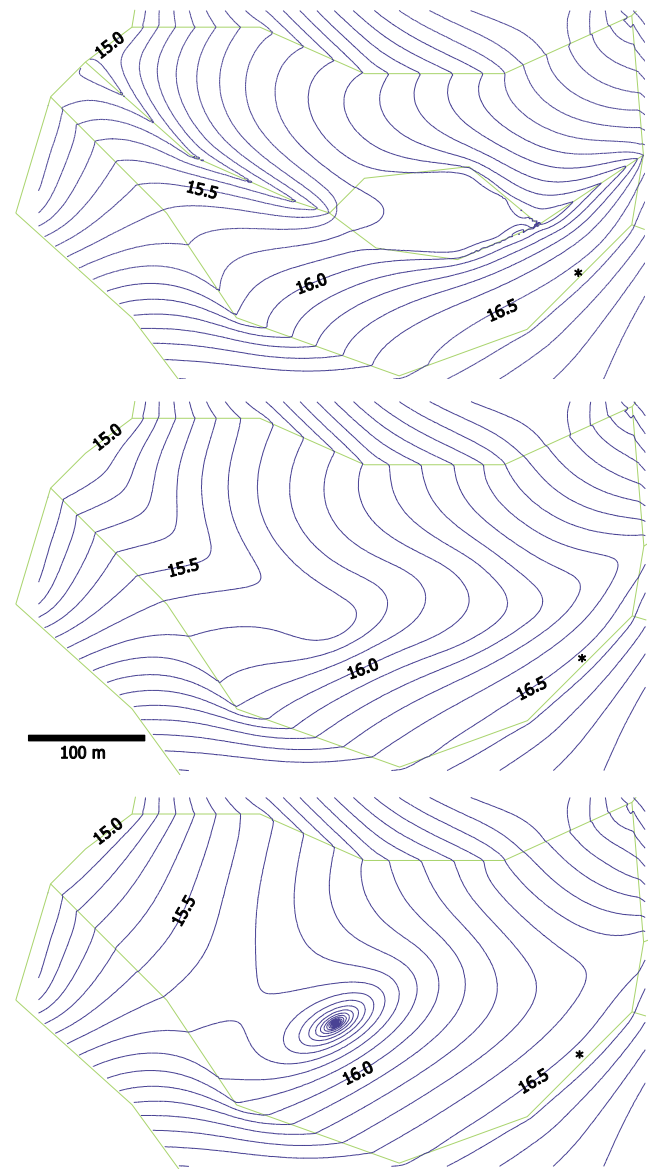


Figure 8. Model-simulated heads (blue) in the 3-layer area of the model. (top) Upper layer (subdomains 2 and 3), (middle) middle layer (subdomain 4), (bottom) lower layer (subdomain 5). Contour interval 0.1 m. Line elements shown in green. The asterisk (*) marks the line segment analyzed in Figure 9.

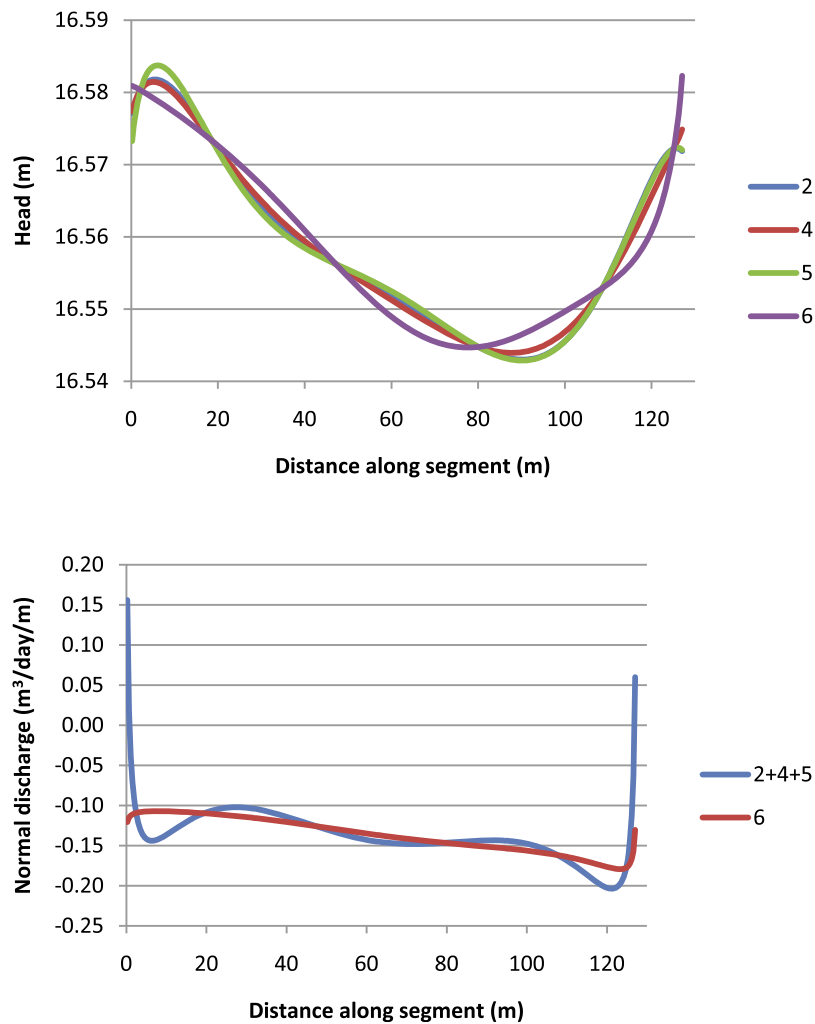


Figure 9. (top) Modeled heads and (bottom) normal component of aquifer discharge along the inter-domain boundary between subdomains 2, 4, 5, and 6. The asterisks in Figure 8 mark the line segment of these graphs. The line elements at this boundary have six degrees of freedom.

[25] Each line element representing an external subdomain boundary or a river has 3 degrees of freedom (unknown strength parameters), while each inter-subdomain line element has 6 degrees of freedom. Along the top edge of the model, the normal-flux boundary has a specified normal component of flux of $0.01 \text{ m}^3/\text{day}/\text{m}$ into subdomains 1 and 7. At the bottom edge of the model, zero normal flux is specified in subdomains 6 and 7. At the left edge of the model, a head of 15 m is specified in subdomains 1, 2, 4, 5, and 6. At the right edge of the model, a head of 20 m is specified in subdomain 7. The river line elements in subdomains 2 and 7 allow head-dependent flux out of or into the model.

[26] The uniform recharge rates specified in subdomains 1, 2, 6, and 7 are listed in Table 1. In subdomain 3 there is no recharge, but there is spatially variable leakage to an overlying pond which has a head of 15.8 m.

[27] In subdomains 2–5, multiquadric extraction elements approximate the spatial distribution of extraction due to recharge and leakage. The leakage fluxes, heads, and extraction rates are all exact at the element basis points and approximated between them. The locations of the basis

points (+), as well as the line element collocation points (x) in this area are shown in Figure 6. These basis point locations apply in all three model layers. The extraction basis points were placed uniformly on hexagonal centers within subdomains and at higher density near the well and surface waters. The density of basis points was selected so that the spacing between them was everywhere less than 1.5 times the leakage factor [Verruijt, 1970] for all layers (see *Strack and Jankovic* [1999] or *Hansen* [2002] for discussions of basis point spacing). The spacing of basis points ranged from 1.0 m in a small zone around the well to 23 m far from the well, river, or pond.

[28] The entire model generated a system of 3032 boundary condition equations corresponding to 3032 unknown element strength parameters. The system of equations was solved with a direct LU decomposition solver in five iterations. Iterations were necessary due to non-linear head-dependent equations in unconfined subdomains. In this example, iteration terminated when the last iteration caused no more than a 10^{-6} fractional change in any element strength parameter. Assembling the equations took 7.1 s on the first iteration and 3.0 s on subsequent iterations using a

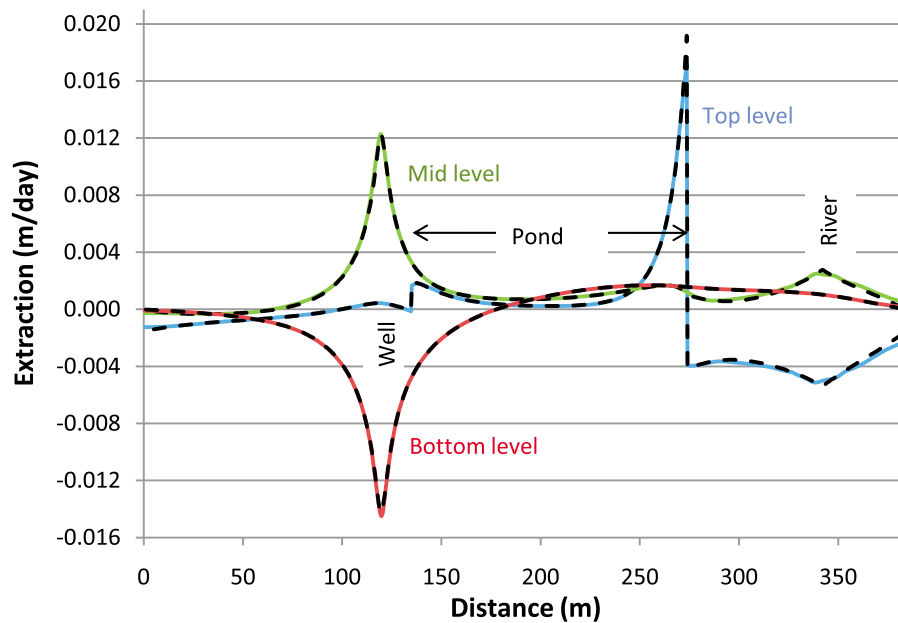


Figure 10. Comparison of steady modeled extraction and extraction based on head differences along transect A–A' shown in Figure 6. The colored solid lines are the modeled extraction computed with equation (13) and the black dotted lines are the extractions computed with equation (6).

personal computer with a dual-core 2.4 GHz processor. Each LU solve of the system took 1.7 s. The total time to solve with five iterations was 29 sec. Because of the subdomain approach, the coefficient matrix resulting from the system of equations is somewhat sparse, containing 42% zeros. The zeros could afford computational efficiencies with a solver that takes advantage of them, although this solver did not.

[29] Model-simulated heads are shown in Figures 7 and 8. These plots were generated by evaluating $h(\Phi(z))$ at a large number of points (40,000) and then contouring this data. Evaluating the solution at 40,000 points took 16 s. Figure 7 shows the modeled heads at the uppermost layer in the whole modeled area, which includes subdomains 2 and 3 in the multilayer part of the model. The contours indicate close approximation of head continuity at inter-subdomain boundaries. Figure 8 shows close-ups of the head patterns in the 3-layer portion of the model. The patterns show the impact of discharges to surface waters and to the well in anisotropic subdomain 5.

[30] As is typical of AE models, the specified boundary conditions were met within extremely small tolerances at all collocation points and ΔQ line intervals associated with inter-subdomain and specified normal flux boundaries. The quality of the inter-subdomain boundary condition approximation is illustrated in Figure 9, which shows the distribution of head and the normal component of discharge along one segment of the boundary between subdomains 2, 4, 5 in the 3-layer part of the model and abutting subdomain 6 in the single-layer part of the model. The continuity of head was perfect at the six collocation points and head discrepancies between collocation points were small, nowhere more than 0.01 m. The continuity of flux across the boundary is perfect for six separate intervals of this line segment as a result of the boundary condition equations. At points along

the segment, the normal component of flow is only approximately continuous. The deviations in the normal component of flow only have local impacts, since there is precise discharge continuity across the six intervals on this segment. The inter-subdomain boundary conditions can be approximated better using line elements with more degrees of freedom [Jankovic and Barnes, 1999].

[31] In the multilayer part of the model, the governing differential equation is met exactly at basis points but only approximated between basis points. Figure 10 shows a check of the accuracy of this approximation, comparing the modeled extraction computed with equation (13) (colored lines) to the extraction computed with equation (6) and modeled heads (black dotted lines) along transect A–A' in Figure 6. The results indicate a very close agreement and good approximation of the differential equation. The poorest approximation is out near the ends of the transect, where the basis point spacing is larger.

[32] A transient case of this model was run, using the steady case described above for the initial head condition. The well in subdomain 5 is shut off at the start of the transient run. Spatially variable extraction elements were added on 50 m centers throughout subdomains 1, 6, and 7 so that extraction due to storage changes could be simulated throughout the entire model. The model was run for ten time steps over a two-day period, with each time step 1.4 times longer than the prior step. The transient evolution of heads along transect A–A' in subdomain 5 is illustrated in Figure 11. Figure 11 also shows the quality of the approximation of the differential equation along this transect at the end of the first four time steps. The plot indicates very close approximation of the differential equation, even near the well at early times, when there is high extraction due to water entering storage.

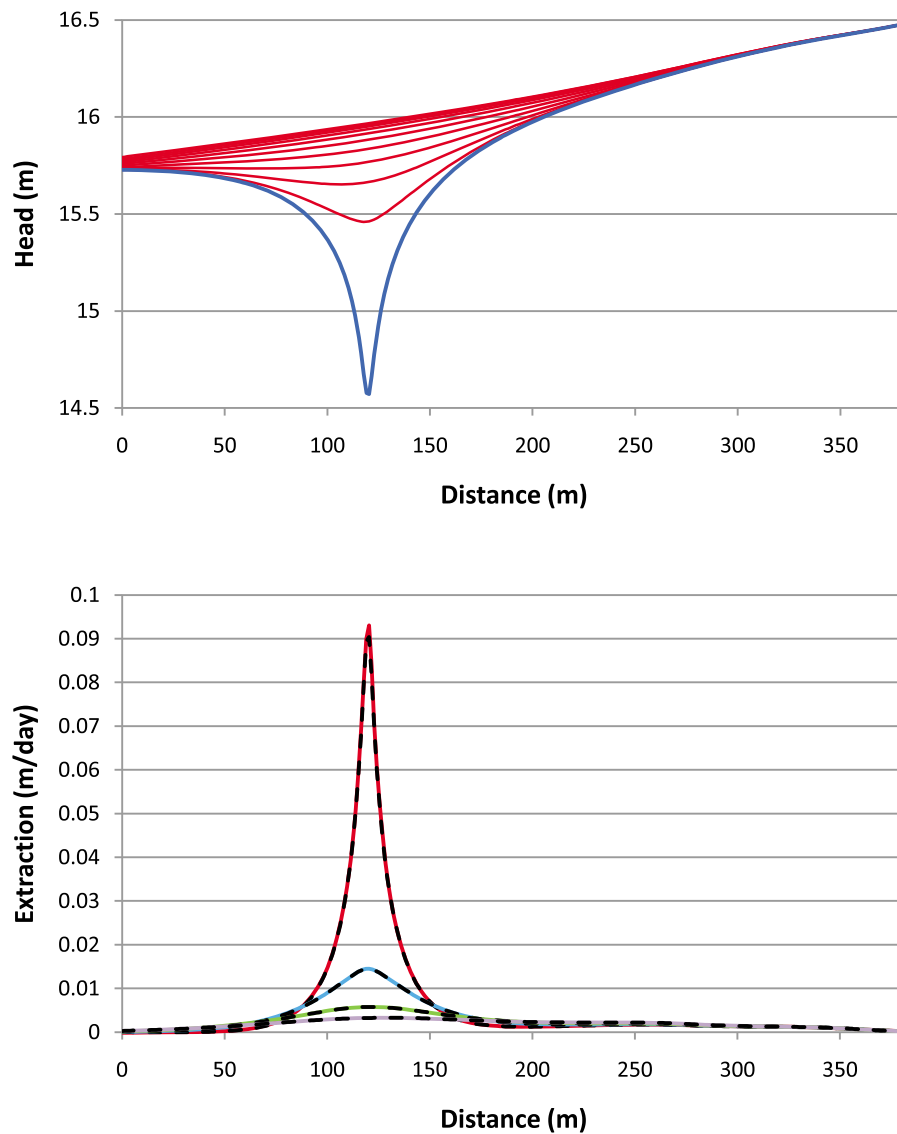


Figure 11. (top) Transient head profiles in subdomain 5 along transect A–A' shown in Figure 6. Initial heads are shown in blue and transient heads shown in red at the following times (days): 0.029, 0.069, 0.125, 0.204, 0.314, 0.468, 0.683, 0.985, 1.41, 2.0. (bottom) Transient model extraction in subdomain 5 along transect A–A'. The colored solid lines are the modeled extractions computed with equation (13) and the black dotted lines are the extractions computed with equation (6). Curves are shown for the first four time steps.

[33] This technique was also checked against the USGS MODFLOW finite difference program [Harbaugh *et al.*, 2000] in a model with simple rectangular geometry, multiple layers, four subdomains with variations in anisotropy, and transient flow. The grid spacing in the MODFLOW model was comparable to the spacing between extraction basis points with this approach. The two approaches yielded nearly identical results for spatial and temporal head distributions.

6. Discussion

[34] The example model demonstrates that the subdomain approach can simulate moderately complex systems with heterogeneity, multiple layers, and variable anisotropy. The boundary conditions at inter-subdomain boundaries can be

met with reasonable accuracy, and the differential equation can be approximated well with a sufficient density of extraction basis points.

[35] The subdomain approach presented here provides a useful extension of the AE method. It adds the ability to model regions with anisotropic media that are also heterogeneous in the ratio and direction of the anisotropy. Such variations in anisotropy are often controlling factors in problems involving seepage through embankments or flow in fractured rock. This approach also allows the model's layering scheme to vary; there can be more layers in the area of interest than in distant areas, efficiently concentrating layering detail only where it is needed and warranted by data.

[36] Another advantage is that subdomain boundary elements may serve multiple purposes, helping reduce the size

of the system of equations. For example, an inter-domain boundary could also serve as the abrupt margin of a spatially variable area sink and as a specified-flux boundary (e.g. an impermeable slurry wall). With infinite-domain AE approaches, multiple elements are typically required for these purposes. Another benefit is that once a solution is in hand, computation of heads and discharges for post-processing is quicker since the subdomain equations for potential and discharge are shorter than infinite-domain equations. A final benefit is that the resulting coefficient matrix is somewhat sparse, which means less computation is needed to assemble the coefficient matrix. While not exploited here, this could lead to computational savings with a solver that exploits the zero coefficients.

[37] Compared with infinite-domain AE approaches, there are some minor drawbacks. One is that at heterogeneity boundaries there is only piecewise continuity of flow across intervals. As the example demonstrated, this drawback can be minor in a well-conceived model. Another drawback is that this approach generates equations for continuity of flow at heterogeneity boundaries whereas no such equations are needed in infinite-domain models. In the example model, this requirement contributed 102 equations to the 3032 total equations (3.4% of all equations), a relatively small incremental cost.

[38] As the example demonstrates, solving the entire system with a direct solver is reasonably quick for a system of several thousand equations. With substantially larger systems, this wouldn't be the case and a different solution scheme might be more efficient. One alternative would be to solve the entire system with an iterative solver [Barrett et al., 1993] instead of a direct solver. This has not been tried here, but iterative solvers can be more efficient than direct solvers for large and sparse systems. Another alternative would be to solve subsets of the entire system and iterate to achieve convergence, an approach that would take advantage of the sparseness of the entire system of equations. Solving element-by-element worked well in systems involving mostly line doublet or line dipole elements [Jankovic and Barnes, 1999], but when tried here with numerous source/sink elements, convergence was poor. Solving domain-by-domain was also tried here with mixed results. Most cases converged, but convergence was less dependable with multilayered systems. This option may warrant further exploration, trying different ways to organize the equations for each domain and various schemes for updating coefficients at each iteration.

[39] **Acknowledgments.** I am grateful to the University of Southern Maine for providing me a semester sabbatical to pursue this research and to the Maine Technology Institute for providing Seed Grant SG3878 to help purchase graphics and numerical libraries for this project. The comments of reviewers James Craig, Henk Haitjema, and a third anonymous reviewer were very thoughtful, detailed, and constructive. Their suggestions were a great help in focusing and clarifying the paper.

References

Bakker, M. (2006a), An analytic element approach for modeling polygonal inhomogeneities in multiaquifer systems, *Adv. Water Resour.*, 29, 1546–1555.

- Bakker, M. (2006b), Analytic element modeling of embedded multiaquifer domains, *Ground Water*, 44(1), 81–85.
- Bakker, M., and K. Hemker (2002), A Dupuit formulation for flow in layered, anisotropic aquifers, *Adv. Water Resour.*, 25, 747–754.
- Barrett, R., M. W. Berry, T. F. Chan, J. Demmel, J. Donato, J. Dongarra, V. Eijkhout, R. Pozo, C. Romine, and H. van der Vorst (1993), *Templates for the Solution of Linear Systems: Building Blocks for Iterative Methods*, 2nd ed., Soc. for Indust. and Appl. Math., Philadelphia, Penn.
- Bear, J. (1972), *Dynamics of Fluids in Porous Media*, Dover, New York.
- Beer, G., I. Smith, and C. Duenser (2008), *The Boundary Element Method With Programming: For Engineers and Scientists*, Springer, New York.
- Bruch, E., and A. Lejeune (1989), An effective solution of the numerical problems at multi-domain points for anisotropic Laplace problems, in *Advances in Boundary Elements*, vol. 2, *Field and Flow Solutions*, edited by C. A. Brebbia and J. J. Connor, pp. 3–14, Comput. Mech., Boston.
- Craig, J. R. (2005), Contaminant transport modeling using analytic element flow solutions, Ph.D. thesis, State Univ. of New York at Buffalo, Buffalo.
- Craig, J. R., I. Jankovic, and R. Barnes (2006), The nested superblock approach for regional-scale analytic element models, *Ground Water*, 44(1), 76–80.
- Fitts, C. (1985), Modeling aquifer inhomogeneities with analytic elements, MS thesis, Univ. of Minn., Minneapolis.
- Fitts, C. R. (2002), *Groundwater Science*, Academic, San Diego, Calif.
- Fitts, C. R. (2004), Discrete analytic domains: A new AEM formulation for modeling anisotropy and heterogeneity, paper presented at EPA/NGWA Fractured Rock Conference, Portland, Maine.
- Fitts, C. R. (2006), Exact solution for two-dimensional flow to a well in an anisotropic domain, *Ground Water*, 44(1), 99–101.
- Haitjema, H. (1995), *Analytic Element Modeling of Groundwater Flow*, Academic, San Diego, Calif.
- Haitjema, H. M., and V. A. Kelson (1996), Using the stream function for flow governed by Poisson's equation, *J. Hydrol.*, 187, 367–386.
- Haitjema, H. M., and O. D. L. Strack (1985), An initial study of thermal energy storage in unconfined aquifers, *Tech. Rep. PNL-5818 UC-94e*, Pac. Northwest Lab., Battelle Mem. Inst., Richland, Wash.
- Hansen, D. (2002), Analytic modeling of leakage in confined aquifer systems, MS thesis, Univ. of Minn., Minneapolis.
- Harbaugh, A. W., E. R. Banta, M. C. Hill, and M. G. McDonald (2000), MODFLOW-2000, the U.S. Geological Survey modular ground-water model: User guide to modularization concepts and the ground-water flow process, *U.S. Geol. Surv. Open File Rep.*, 00-92, 121 p.
- Jankovic, I., and R. Barnes (1999), High-order line elements in modeling two-dimensional groundwater flow, *J. Hydrol.*, 226, 211–223.
- Kythe, P. K. (1995), *An Introduction to Boundary Element Methods*, CRC Press, Boca Raton, Fla.
- Liggett, J. A., and P. L-F. Liu (1983), *The Boundary Integral Equation Method for Porous Media Flow*, Allen and Unwin, London.
- Muskat, M. (1937), *The Flow of Homogeneous Fluids Through Porous Media*, McGraw-Hill, New York.
- Shiah, Y. C., P. Hwang, and R. Yang (2006), Heat conduction in multiply adjoined anisotropic media with embedded point heat sources, *J. Heat Transfer*, 128, 207–214.
- Strack, O. (1989), *Groundwater Mechanics*, Prentice Hall, Englewood Cliffs, N. J.
- Strack, O. (2003), Theory and applications of the analytic element method, *Rev. Geophys.*, 41(2), 1005, doi:10.1029/2002RG000111.
- Strack, O. D. L., and H. M. Haitjema (1981), Modeling double aquifer flow using a comprehensive potential and distributed singularities: 2. Solution for inhomogeneous permeability, *Water Resour. Res.*, 17(5), 1551–1560.
- Strack, O., and I. Jankovic (1999), A multi-quadric area-sink for analytic element modeling of groundwater flow, *J. Hydrol.*, 226, 188–196.
- Strack, O., I. Jankovic, and R. Barnes (1999), The superblock approach for the analytic element method, *J. Hydrol.*, 226, 179–187.
- Verruijt, A. (1970), *Theory of Groundwater Flow*, Macmillan, London.

C. R. Fitts, Geosciences Department, University of Southern Maine, Gorham, ME 04038, USA. (cfitts@usm.maine.edu)